International Journal of Steel Structures
https://doi.org/10.1007/s13296-022-00610-5

Online ISSN 2093-6311
Print ISSN 1598-2351

Optimal Procedure for Determining Constitutive Parameters of Giuffrè–Menegotto–Pinto Model for Steel Based on Experimental Results

Van Tu Nguyen[1] · **Xuan Dai Nguyen**[1]

Received: 11 January 2022 / Accepted: 21 April 2022

Abstract
Describing the nonlinear behaviour of constitutive materials plays an important role in structural analysis. The Giuffrè–Menegotto–Pinto (GMP) model is widely used in the nonlinear modelling of steel structures, with its constituent parameters often calibrated from tests. However, the experimental results obtained require intermediate identification procedures before being used directly, meanwhile, the calibration of model parameters based on experimental data is complicated due to the many interrelated constituent variables. This paper aims to propose a method that calibrates the GMP model parameters optimally based on the experimental data. An available set of test results of high-strength steels subjected to cyclic strain is employed to perform an optimal analysis. The obtained results are then compared to numerical and experimental results to evaluate the effectiveness of the proposed method. An extensive study was carried out to evaluate the applicability of the optimal parameters obtained and those suggested by OpenSees. The findings reveal that the proposed procedure is highly efficient, making it a useful option for developing OpenSees applications that automatically calibrate model parameters. A typical 3D steel frame structure subjected to an earthquake is analyzed to evaluate the applicability of the results obtained.

Keywords Giuffrè–Menegotto–Pinto model · Optimal analysis method of parameters · Optimally calibrated model · Cyclic behaviour · OpenSees

1 Introduction

In recent years, steel structures have been increasingly used in construction engineering. Based on the numerous undeniable benefits and high stability at a reasonable cost, they have become the preferred structural solutions and functional devices in design, especially for large-scale structures located in seismic regions.

High-strength and low-strength steel (i.e., low carbon steel) are two common types of steel that have been widely used in construction engineering with different functions and roles, depending on the representative structural element. Based on many outstanding advantages, high-strength steel is known as one of the most commonly used steels for structures. It facilitates creating structures that are relatively both stronger and lighter than other traditional structures such as concrete, wood, etc. Consequently, it not only reduces the size and weight of structures but also allows the opening of large spaces with high performance and sustainability. Further, it offers flexible adaptation as it can be pre-manufactured in various sizes, resulting in quick installation and construction. Meanwhile, low carbon steel is considered a functional material that is commonly used in seismic design based on its great ductility. As a result, it's used in advanced seismic technologies, typically as additional energy dissipation devices for structures to provide seismic protection.

Nonlinearities are common in most applications involving steel structures, especially when the structures are subjected to severe impacts such as strong earthquakes. Specifically, the nonlinear behaviours can occur in some specific structural components (performance-based seismic design), supplementary devices, or both, all of which play important

✉ Xuan Dai Nguyen
xuandai.nguyen@lqdtu.edu.vn

Van Tu Nguyen
nguyentu@lqdtu.edu.vn

[1] Present Address: Institute of Techniques for Special Engineering, Le Quy Don Technical University, Hanoi, Viet Nam

Published online: 10 May 2022

components in dissipating energy through inelastic deformations inside structures and/or devices. Therefore, the nonlinear behaviour of steel materials has always been a topic of high interest in recent decades (Anderberg, 1988; Chan et al., 2013; Cofie & Krawinkler, 1985; Dai Nguyen & Guizani, 2021; Dunne & Petrinic, 2005; Garivani et al., 2016; Myers, 2009; M. Wang, Fahnestock, et al., 2017; Wang, Li, et al., 2017; Ziemian, 1990).

In order to investigate the nonlinear response of materials and structures, two fundamental methodologies, including tests and numerical modelling, are commonly performed. Due to high costs and limited conditions, tests are mainly conducted on specific structural components or small-scale structures. In such a context, the numerical analysis method seems to be the most effective solution where the nonlinear time-history analysis is widely employed, especially to investigate the nonlinear responses of structures subjected to earthquakes. Therefore, current seismic design codes consider this methodology to be an effective and reliable method for seismic study (AASHTO, 2017; ASCE/SEI-41–13, 2014; CSA-S6, 2019; ECS, 2005a; NRCC, 2015; TCVN-9386:, 2012, 2012). In addition, the great development of structural analysis software has provided many effective solutions to employ nonlinear analyses. However, despite the undeniable advantages of numerical approaches, the accuracy of numerical analyses is strongly dependent on the fit that can describe the behaviour of constitutive materials. In other words, the accordance between the numerical model and the real structural model. The behaviour of materials is consequently considered a key parameter and it can only be determined by tests to identify the constitutive parameters for numerical models.

Generally, the fundamental method to define the behaviour of steels is to conduct experimental studies of representative steel specimens by uniaxial tests under two typical loading scenarios, including monotonic loading and cyclic loading, corresponding to the behaviour of the structure in terms of static and cyclic dynamic loads. Research on the monotonic behaviour of steel have been investigated over the years, the obtained results allowed to provide analytical models of materials. Anderberg (1988) recognized that an analytical description of the stress–strain behaviour is essential, especially in numerical modelling solutions. Accordingly, the experimental method used to determine the strength properties is of great importance to obtain accurate results. Based on the model of Ramberg and Osgood (1943), the authors developed a simplified model based on expressing the deformation transition via three components (Young's modulus and two secant strengths) that are separately obtained from different monotonic tests. Real et al. (2014) investigated the difference between various nonlinear behaviour models of stainless steel using monotonic test data. The authors developed an interactive computer program to analyse the available experimental data which allows determining the essential parameters for the expression of the analytical model for various stainless steels.

On the other hand, according to obtained results of experimental studies on the nonlinear behaviour of steel structures, the cyclic loading offers a significant alteration in the behaviour of the steel structure compared with the monotonic loading (Hai et al., 2018; M. Wang, Fahnestock, et al., 2017; Wang, Li, et al., 2017). In addition, the cyclical feature of steel structures has been carried out and widely applied over decades, especially for the systems exhibiting nonlinear responses under seismic impacts (Aghlara & Tahir, 2018; Campbell & Co-auteur, 1970; Dai Nguyen & Guizani, 2021; Jamkhaneh et al., 2019; Saeedi et al., 2016; Ziemian, 1990). Based on the obtained experimental results, numerous observed cyclical behaviours of steel structures have been investigated and developed into a series of constitutive models with different degrees of compatibility (Bouc, 1967; Chaboche, 1986; Giuffrè, 1970; Hu & Shi, 2018; Menegotto & Pinto, 1973; Takeda et al., 1970; Y.-B. Wang, Fahnestock, et al., 2017; Wang, Li, et al., 2017; Wen, 1976). In general, these proposed models are developed based on the obtained cyclic stress–strain relationship from extensive experimental studies. They generally concern the Bauschinger effect and kinematic/isotropic hardening behaviour, which both are important aspects of the overall cyclic loading history (Bauschinger, 1886; Myers, 2009).

Further, these models are phenomenologically established rather than being constructed on the basis of mechanical principles where their characteristics are considered by some typical parameters making them as generic as possible in order to match a variety of experimentally observed behaviours. Specifically, based on the available data on the stress–strain relationship of structures, essential parameters for commonly used constitutive models are determined (Hu & Shi, 2018; M. Wang, Fahnestock, et al., 2017; Wang, Li, et al., 2017). In the context of the increasing use of numerical approaches in structural analysis, these models are useful in predicting the nonlinear behaviour of structures in a realistic manner.

In practice, the experimental data can be generated from pre-planned testing and/or publicly available datasets. The calibration process is then carried out by looking for a set of model parameters that match the analytical results and the experimental test as accommodating as possible (Anderberg, 1988; Hai et al., 2018; Hu & Shi, 2018; Real et al., 2014; M. Wang, Fahnestock, et al., 2017; Wang, Li, et al., 2017; Y.-B. Wang, Fahnestock, et al., 2017; Wang, Li, et al., 2017). Several studies have used such models in analysis to evaluate the nonlinear behaviour of structures (Dai Nguyen & Guizani, 2021; Hai et al., 2018; Sheikhi & Fathi, 2020; Taiyari et al., 2019; M. Wang, Fahnestock,

et al., 2017; Wang, Li, et al., 2017). Typically, some studies compare the specific models to explore the applicability of each one for the considered steel structure (Hai et al., 2018; Real et al., 2014). The remaining problem is that the parameters of the selected model have not been calibrated in an optimal way, leading to potential errors in evaluating its proper applicability (Hai et al., 2018) as well as the reliability of analysis results.

Logically, the accuracy of numerical analysis responses is driven by the applicability of the equivalent model utilized. In the past decades, although several phenomenological models have been carried out alongside with equivalent calibrated models, the concordance of numerical models with experimental tests still has shortcomings, and the optimal analysis of the model parameters to improve the accuracy of numerical analyses has received insufficient attention. Consequently, optimal identification of the essential parameters for the representative model of the structure's behaviour is an important phase of structural analysis calibration, allowing the most approximate reflection of the material behaviour of the real structure while increasing the accuracy and efficiency of subsequent numerical analyses.

In the current context of performance-based seismic design, numerical simulation has increasingly become an effective method. The majority of the numerical studies were conducted using commercial software with high performance and accuracy in structural analysis, which effectively represented various material behaviour models. Practically, typical nonlinear behaviours of steel have been integrated into commercial structural analysis programs such as Abaqus (Abaqus, 2014), ANSYS (ANSYS, 2021), SAP2000 (SAP2000, 2020), etc., which offer a large library of finite elements and great GUIs to enable an efficient and detailed modelling. However, due to their limited scalability and high investment costs, they are out of reach for most researchers.

The Open System for Earthquake Engineering Simulation (OpenSees) of Pacific Earthquake Engineering Research (PEER) Center (OpenSees, 2020) is one of the most widely used open-source software for studying the structure subjected to earthquakes with a variety of material behaviour models and analysis methods. It offers a potential solution in the form of a community-owned research code with significant and expanding modelling capabilities, as well as a larger possibility for research and development initiatives to last longer. In addition, it allows the integration of extensive tools for processing experimental results, resulting in not only a reduction in intermediate steps but also an increase in the efficiency of analyses. With many undeniable advantages, OpenSees is increasingly used in the seismic-resistant design. Specifically, OpenSees has a variety of steel models, including the Giuffrè-Menegotto-Pinto model (Giuffrè, 1970; Menegotto & Pinto, 1973), which is one of the most extensively utilized for seismic analysis steel structures (Bosco et al., 2016; OpenSees, 2021).

This paper aims to perform an optimal procedure that is integrated into OpenSees, to calibrate the Giuffrè-Menegotto-Pinto (GMP) model for the cyclic nonlinear behaviour of steel from the experimental tests.

To this end, the description of the GMP model integrated into OpenSees is first outlined. The proposed procedure for optimal identification and analysis of the model's parameters is presented. The proposed method is then evaluated by a comparison between the optimally calibrated model with available experimental results and available non-optimal models of typical high-strength steels. An extensive study using the values recommended by OpenSees for critical parameters to evaluate the convenience appropriateness of the suggested values and the effectiveness of the optimally calibrated model. The obtained parameters for specific high-strength steel are then assigned to a typical steel structure subjected to earthquakes to investigate the applicability of the proposed method.

2 Overview the Giuffrè–Menegotto–Pinto (GMP) Model

The GMP model, which was first developed by Giuffrè (1970), is based on Goldberg and Richard's nonlinear stress–strain relationship (Goldberg & Richard, 1963) and integrates the influence of inelastic deformations on the Bauschinger effect (Bauschinger, 1886) observed from tested steel specimens. Namely, Giuffrè proposed a set value of parameters for the constitutive model based on the obtained response of cyclic stress–strain relation derived from the test of a single 10-mm-diameter specimen subjected to symmetric tension–compression cycles, which was further improved by Menegotto and Pinto (Menegotto & Pinto, 1973). The hysteretic behaviour of the GMP model is illustrated in Fig. 1.

The expression of the GMP model is assumed as the following:

$$f* = b\varepsilon* + \frac{(1-b)\varepsilon*}{\left(1+|\varepsilon*|^{R}\right)^{1/R}} \tag{1}$$

f^* and ε^* are the normalized stress and strain that are determined as the equation (2) follows:

$$f* = \frac{f-f_r}{f_0-f_r}; \varepsilon* = \frac{\varepsilon-\varepsilon_r}{\varepsilon_0-\varepsilon_r} \tag{2}$$

f, ε) are the stress–strain at the considering state; (f_0, ε_0) are the yield stress and yield strain, respectively; (f_r, ε_r) are

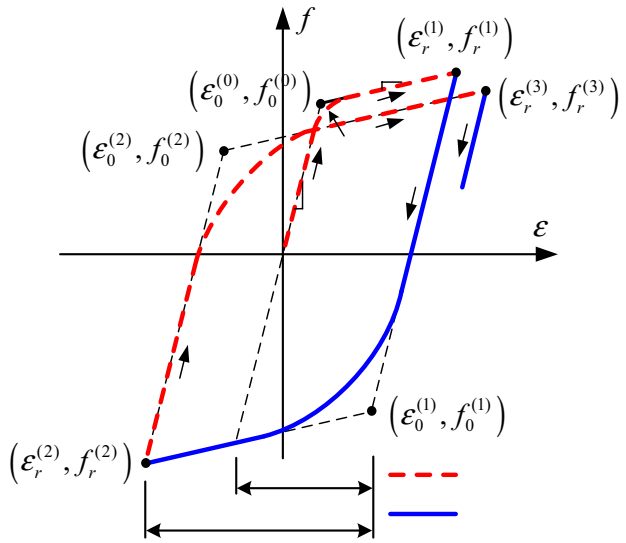

Fig. 1 Hysteretic behaviour of Guiffre-Menegotto-Pinto model

the stress and strain at the reserve point (see in Fig. 1); R is the parameter to control the smoothness of the transition from elastic to a plastic state, includes the Bauschinger effect. This parameter is dependent on the peak deformation correlation between the latest yield point and the maximum plastic deformation in the load direction after reversing, expressed as below:

$$R = R_0\left(1 - \frac{CR_1.\xi}{CR_2 + \xi}\right) > 0 \tag{3}$$

R_0 is the value of R during first loading; CR_1 and CR_2 are experimentally determined parameters that are used to define the behaviour of material;

ξ is the normalized plastic deformation range controlling R, which is updated after a reversal in strain. The definition of ξ is expressed as follows:

$$\xi = \left|\frac{\varepsilon_p - \varepsilon_0}{\varepsilon_y}\right| \tag{4}$$

ε_y is the initial yield strain, ε_0 is the yield strain at the current loading process, and ε_p is the maximum strain in the load direction. The parameters f_0, ε_0, f_r, ε_r, and R are updated after each strain reversal.

The position of the yield surface is assumed to be fixed in the above model. That means the isotropic hardening behaviour has not been considered. In OpenSees, for the uniaxial material Steel02 model (OpenSees, 2020), the isotropic hardening effect is implemented by two states of tension (f_{st}) and compression (f_{sc}) respectively expressed as the following equations:

$$f_{st} = f_y a_3\left[\frac{\varepsilon_p^{\max} - \varepsilon_p^{\min}}{2a_4\varepsilon_y}\right]^{0.8}; f_{sc} = f_y a_1\left[\frac{\varepsilon_p^{\max} - \varepsilon_p^{\min}}{2a_2\varepsilon_y}\right]^{0.8} \tag{5}$$

f_y and ε_y are the initial yield stress and strain, respectively; $\varepsilon_p^{\min}$ and $\varepsilon_p^{\max}$ are the minimum and maximum strain values, recorded for each loading direction; a_1, a_2, a_3, a_4 are four isotropic hardening parameters.

In recent decades, the GMP model has become one of the most popular models applied in modelling the nonlinear behaviour of steel structure (Bosco et al., 2016; Bu et al., 2021; Hai et al., 2018; Zhuge et al., 2022).

3 Calibration of the Model and Proposed Optimization Process

3.1 Proposed Optimal Calibration Method

As discussed above, the calibration procedure aims to determine the model's parameters so that the numerical model is consistent with the test observations. According to the GMP model, there are a total of ten (10) constitutive parameters that need to be determined. Among them, the elastic modulus E_0 is usually measured from the initial elastic states (first hysteresis loop) by linear interpolation and it is then considered to be constant during the optimization process. The yield strength f_y is approximated by the stresses in the yield plateau region where the stress curve's slope decreases more than 20% from the linear state, based on the criteria proposed by Jiao et al. (2015). The obtained values are then validated by comparing them with the available test results of Hai et al. (2018). Accordingly, the obtained values by the such method are in good agreement with the available test results. The remaining parameters include R_0, b, CR_1, CR_2, a_1, a_2, a_3, a_4 are determined based on the matching criteria of the GMP model.

To do so, an optimal analysis method of parameters is proposed to calibrate the model in order to converge test results to the predicted material hysteretic responses. The normalized least-squares error optimization is employed to minimize the discrepancy between tested and predicted material hysteretic responses, which are expressed as:

$$\text{Error}(\mathbf{x}) = \sqrt{\frac{\sum_{i=1}^{n}\left(f_{test}^{i} - f_{pre}^{i}(\mathbf{x})\right)^2}{\sum_{i=1}^{n}\left(f_{test}^{i}\right)^2}} \tag{6}$$

where, f_{test}^{i} is the test stress at the ith strain step, $f_{pre}^{i}(\mathbf{x})$ is the stress predicted by the material model at the ith strain step, and $\boldsymbol{x}$ is the vector of nine parameters of the GMP model, defined as follows:

$$\mathbf{x} = \left\{ E_0 \;\; b \;\; R_0 \;\; CR_1 \;\; CR_2 \;\; a_1 \;\; a_2 \;\; a_3 \;\; a_4 \right\} \tag{7}$$

In order to calibrate these nine (9) parameters, Optimization Toolbox in Matlab software is employed to find a constrained minimum of a function of multivariable, fmincon (MathWorks, 2020). Namely, the optimization function is determined by equation (6) and the variables are determined by equation (7).

The proposed procedure of calibration and optimal analysis parameter is illustrated in Fig. 2 below:

In general, OpenSees also recommends values for some specific parameters of GMP model as follows: R_0 ranges from 10 to 20; $CR_1 = 0.925$; $CR_2 = 0.15$ (Mazzoni, McKenna, Scott, & Fenves, 2006). The efficiency of these parameters is highly significant in shortening the time of analysis and increasing the convergence in the optimal analysis process because of the considerable reduction of the variable. In order to validate this recommendation, the applicability of these parameters will be investigated in the analysis below.

3.2 Application of the Proposed Model to Calibrate Experimental Results

In this section, a set of available test results, which is performed by Hai et al. (2018) for high strength steel specimens (including four different steel grades such as Q460D, Q550D, Q690D, and Q890D), is employed to evaluate the proposed optimal calibration process to determine the parameters of the GMP model. The names of test specimens are assigned the full specifications of the steel grades, geometrical parameters (the cross-section of specimens), and strain protocols.

The geometrical parameters of considered specimens are detailed in Fig. 3. The research scope focuses on the nonlinear behaviour of the test specimens, so that the two typical smallest cross-sections are of interest, including 10 mm × 10 mm and 16 mm × 16 mm (see in Fig. 3).

These specimens are subjected to cyclic loadings, represented as strain histories with two specific protocols shown in Fig. 4. The strain rate is considered constant and equals to 0.2%/s in order to limit the potential effects of temperature increase due to inelastic strain. The strain protocol SH1 has a constant amplitude of

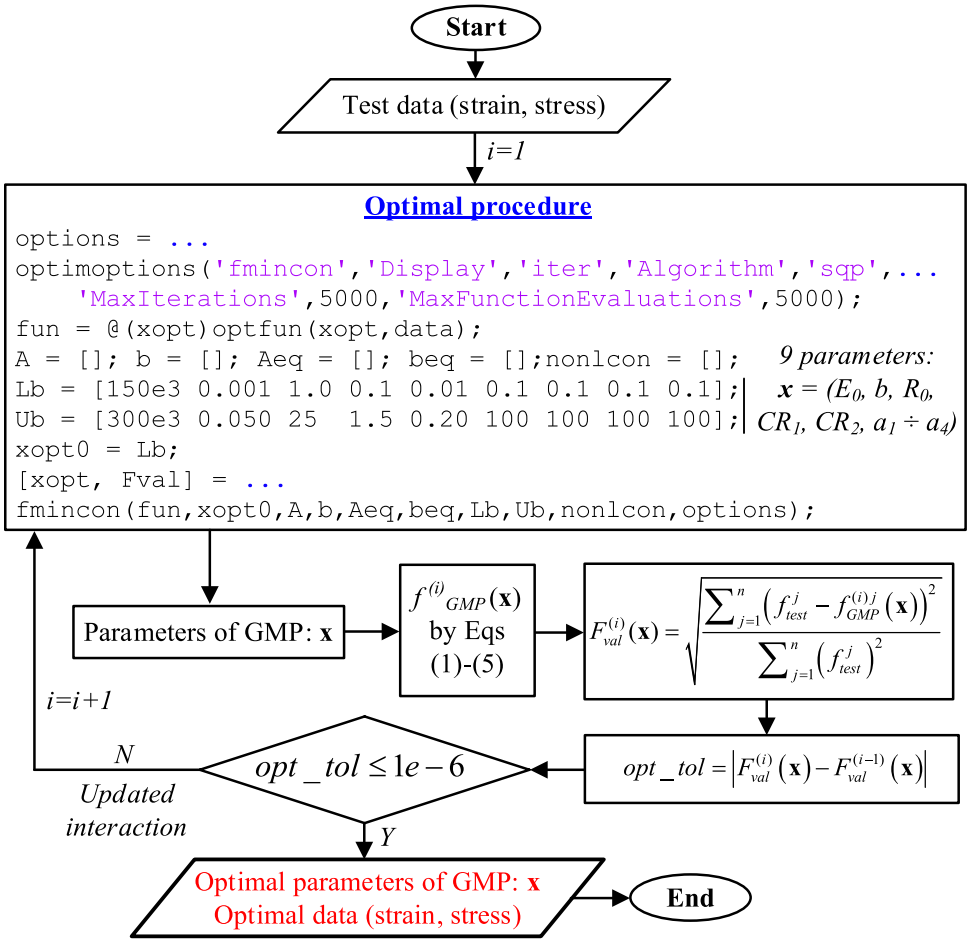

Fig. 2 Block diagram for optimal calibration of GMP model's parameters

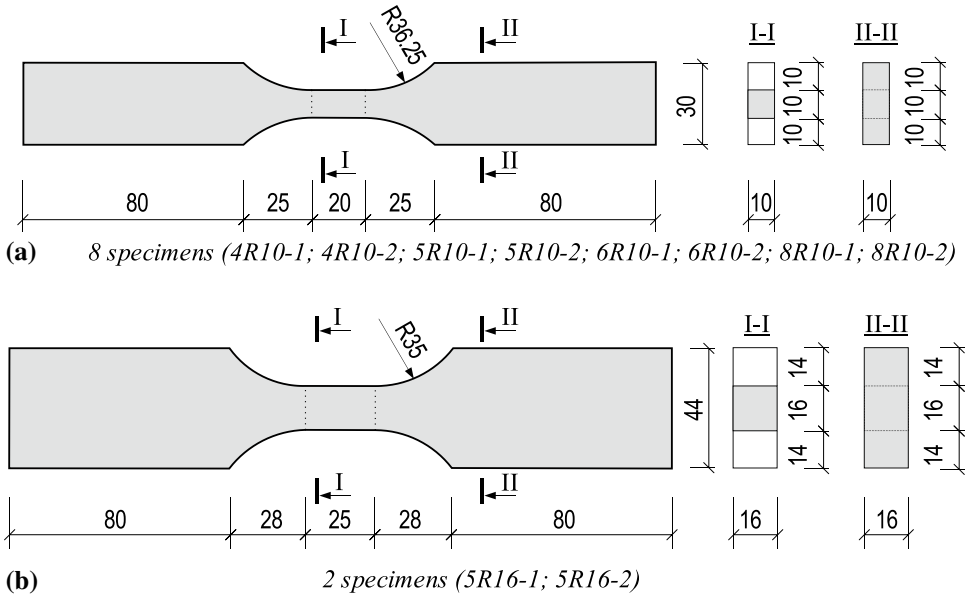

Fig. 3 Geometrical parameters and corresponding specimens (Hai et al., 2018)

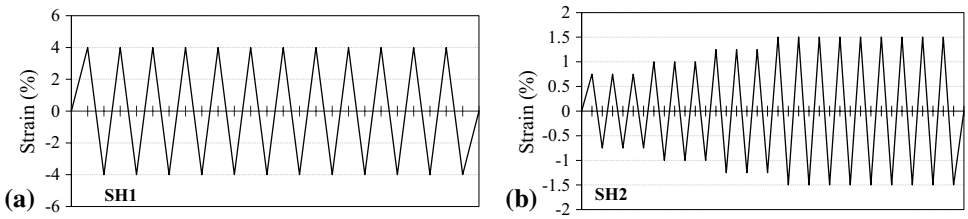

Fig. 4 Cyclic strain histories used for tests: **a** protocol SH1 and **b** protocol SH2 (Hai et al., 2018)

4% (constant strain amplitude test). The strain protocol SH2 has increasing amplitudes of 0.75%, 1%, 1.25%, and 1.5% (variable strain amplitude test) where the first three strain amplitudes are loaded with three cycles (see in * MERGEFORMAT Fig. 4(b)). It should be noted that, the specimens 4R10-1, 5R10-1, 6R10-1, 8R10-1, and 5R16-1 are subjected to strain protocol SH1, the remaining specimens (i.e., 4R10-2, 5R10-2, 6R10-2, 8R10-2, and 5R16-2) are subjected to strain protocol SH2. In the experimental investigation, the specimens are loaded to a failure stage, where the largest amplitudes of strain histories (4% for SH1 and 1.5% for SH2) are maintained until the specimen fails.

However, in the framework of this study, the nonlinear cyclic behaviour is of more interest to determine the constitutive model than the failure mode of the structure. Therefore, a certain number of cyclic loads are considered to reduce the analytical processing and quickly an achieve iteration convergence. To do so, 12 cycles are considered for the protocol SH1 and 18 cycles (includes 03 cycles for each of the first three amplitudes and 09 cycles for the final amplitude) are applied in the protocol SH2 (see in Fig. 4(b)). Accordingly, the instability of test specimens did not affect the analysis results, although it occurs during the last cycles of the test of the specimen 4R10-2, 6R10-2 and 5R16-2 (with more than 400 cycles).

According to the above block diagram (Fig. 2), the constitutive parameters of the GMP model are determined for each test using the developed computer program. The essential parameters of considered materials are optimally identified and presented below in Table 1, where the ErrorVal (%) is calculated by Eq. (6).

As shown in Table 1, there is a slight difference in the main parameters of material between the constant strain amplitude tests (SH1) and those of variable strain amplitude tests (SH2). Namely, the difference in the results of Young's modulus is less than 3.5% (3.41% for specimen 8R10), while the difference in the yield strength is found about 2.8% (specimen 6R10). According to the author's experience, these differences are practically acceptable due to potential mistakes and tolerance that may occur in the processing of experimental tests. On the other hand, the difference in the remaining parameters of the calibrated model seems to be more significant. It can be explained that SH1 has a much larger maximum amplitude than SH2, which leads to significant nonlinear states of constant strain amplitude tests (SH1), resulting in the accumulation of residual deformation by SH2 after each load cycle is smaller than by SH1.

Table 1 The parameters of the Giuffrè-Menegotto-Pinto model for tested specimens

Specimen parameter	4R10-1	4R10-2	5R10-1	5R10-2	6R10-1	6R10-2	8R10-1	8R10-2	5R16-1	5R16-2
E_0 (MPa)	273,800	267,800	222,300	224,500	224,800	218,800	225,600	217,900	201,400	200,300
f_y (MPa)	591.2	595.2	673.3	686.9	801.5	824.3	1048.5	1049.3	645.1	628.1
b	0.013	0.009	0.004	0.003	0.003	0.001	0.003	0.008	0.007	0.043
R_0	17.402	20.000	20.000	14.180	13.385	14.194	20.000	20.000	5.437	7.643
CR_1	0.790	0.910	0.918	0.889	0.872	0.910	0.910	0.895	0.500	0.500
CR_2	0.010	0.119	0.300	0.300	0.300	0.300	0.220	0.124	0.261	0.010
a_1	0.130	0.133	0.003	0.053	0.004	0.226	0.034	0.289	0.192	0.188
a_2	60	60	1	17.22	1	60	7.385	60	60	60
a_3	0.130	0.002	0.003	0.003	0.004	0.004	0.005	0.005	0.192	0.188
a_4	60	1	1	1	1	1	1	1	60	60
ErrorVal (%) =	12.9	2.6	6.0	3.7	6.6	6.8	5.3	3.4	7.1	6.0

Figure 5 shows a comparison of stress–strain relationships between the test results, the available results of Hai et al. (2018) (which are not optimal), and the optimally calibrated model. For constant strain amplitude tests, the transition from plastic to elastic state and vice versa of the optimally calibrated model shows a better match with the test results than that of the non-optimal models. In addition, for the variable strain amplitude test, these obtained results are much more consistent, not only at the transition state but also at the peak values of both strain and stress. This result can lead to a more accurate prediction of energy dissipation capacity due to the inelastic deformation of material by the optimally calibrated model.

In order to evaluate the convenience of the parameter values recommended by OpenSees (Filipou et al., 1983), an extensive analysis is performed on two specimens of 4R10-2 and 5R16-2. Specifically, for each specimen, three values of R_0, including $R_0 = 10$, 15, and 20, are taken into the optimal analysis method of parameters similar to the previous section. The obtained results are shown in Table 2 and Fig. 6.

As can be observed, R_0 seems to be a significant parameter for the fit between the predicted model and test results. The better consistence in this case study corresponds to the higher value of R_0 (in the range of 10 to 20). Furthermore, using the recommended values of OpenSees is difficult to meet the matching criteria. The difference (i.e., ErrorVal) between the test results and the calibrated model is thereby much larger than the optimal one (see in Table 1 and Table 2). In some particular cases, results by using suggested values of OpenSees and test results seem to be identical (as shown in Fig. 6.(e) for $R_0 = 20$), suggesting that the recommended values of OpenSees are reasonable and may be appropriate. But for other cases, it is difficult to achieve a good agreement between the model proposed by OpenSees and experimental results. Despite that observation, the optimally calibrated model is still meaningful when it demonstrates a better match (see in Fig. 6.(f)).

From the above analysis results, the optimally calibrated model is highly consistent with the test results, suggesting that the optimal analysis method of parameters offers great efficiency in identifying and calibrating the parameters of the GMP model from the experimental results of steel cyclic behaviour, and can be extensively used for modelling steel structures with high accuracy.

The proposed method also demonstrates the capability of the GMP model in describing the cyclic nonlinear behaviour of high-strength steel. In the context of using open-source codes, such as OpenSees (OpenSees, 2020), for nonlinear analysis of steel structures, the proposed method offers an effective solution for generating software tools that allow the experimental results to be used as input parameters for numerical analysis with high accuracy.

4 Application in Steel Structure Analysis

4.1 Description of the Considered Structure

In this section, a numerical analysis is performed using OpenSees Navigator (OpenSeesNavigator, 2020) to investigate the behaviour of steel structures of a 5-story building subjected to earthquakes, as illustrated in Fig. 7.

The considered structure is a typical steel frame for a building structure, including five spans in the X direction (5×6.6 m), three spans in the Y direction (3×6.6 m), and five floors (5×4.2 m) (see in Fig. 7). The cross-sections of column and beam systems are W12 × 26 section based on AISC Shapes Database v15.0 (AISC, 2017). The dimensions of W12 × 26 are assigned such as $d = 310$ mm; $b_f = 165$ mm; $t_w = 5.84$ mm; $t_f = 9.65$ mm (see Fig. 8).

The material properties used in the model corresponds to the specimen 4R10-1 from the experimental dataset

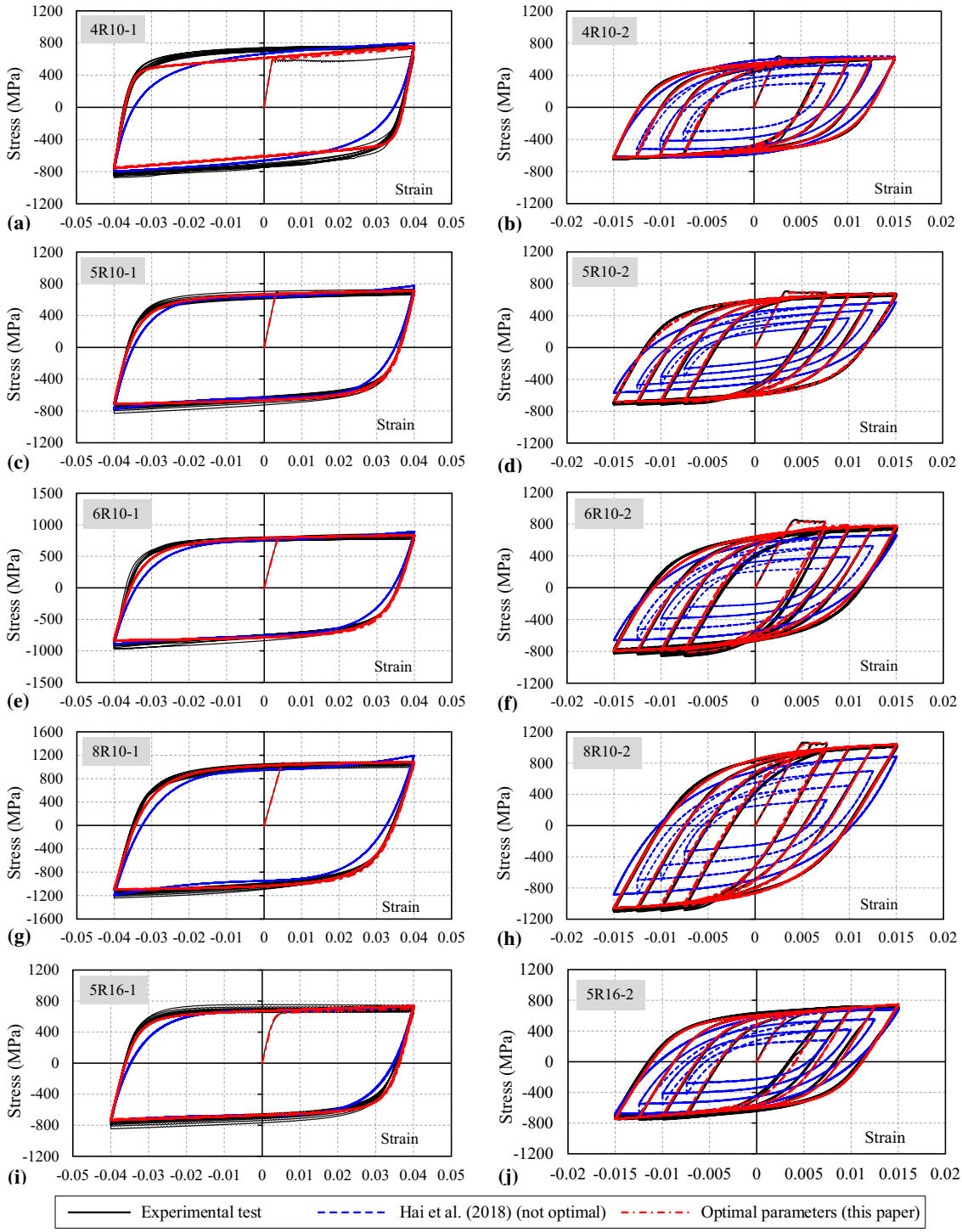

Fig. 5 Comparison among predicted behaviour (this paper), the available experimental studies, and calibration of Hai et al. (2018)

of Hai et al. (2018). The GMP model, represented by the Steel02 model in OpenSees, is employed to model the behaviour of the material. The optimal analysis procedure, as shown in Fig. 2, is used to determine the input parameters of the OpenSees model. Specifically, the optimally calibrated parameters are assigned to the model as the obtained results from Table 1 ($E_0 = 273.8$ GPa, $f_y = 591.2$ MPa, $b = 0.0133$, $R_0 = 17.4$, $CR_1 = 0.79$, $CR_2 = 0.01$, $a_1 = 0.13$, $a_2 = 60$, $a_3 = 0.13$, $a_4 = 60$).

The load applied to the structure includes: the nodal mass of structure 20 kNs^2/m, dead load at nodes 10 kN.

Table 2 The parameters of the GMP model for recommended values of OpenSees

Parameter	Specimen					
	4R10-2			5R16-2		
E_0 (MPa)	267,800	267,800	267,800	200,300	200,300	200,300
f_y (MPa)	595.2	595.2	595.2	628.1	628.1	628.1
b	0.0120	0.0012	0.0047	0.05	0.0266	0.0233
R0	10	15	20	10	15	20
CR1	0.925	0.925	0.925	0.925	0.925	0.925
CR2	0.15	0.15	0.15	0.15	0.15	0.15
a1	0.133	0.133	0.133	0.172	0.188	0.188
a2	60	60	60	54.8	60.000	60.000
a3	0.101	0.093	0.133	0.188	0.188	0.188
a4	45.502	41.840	60	60	60	60
ErrorVal (%)	38.3	16.6	4.9	43.9	26.5	16.2

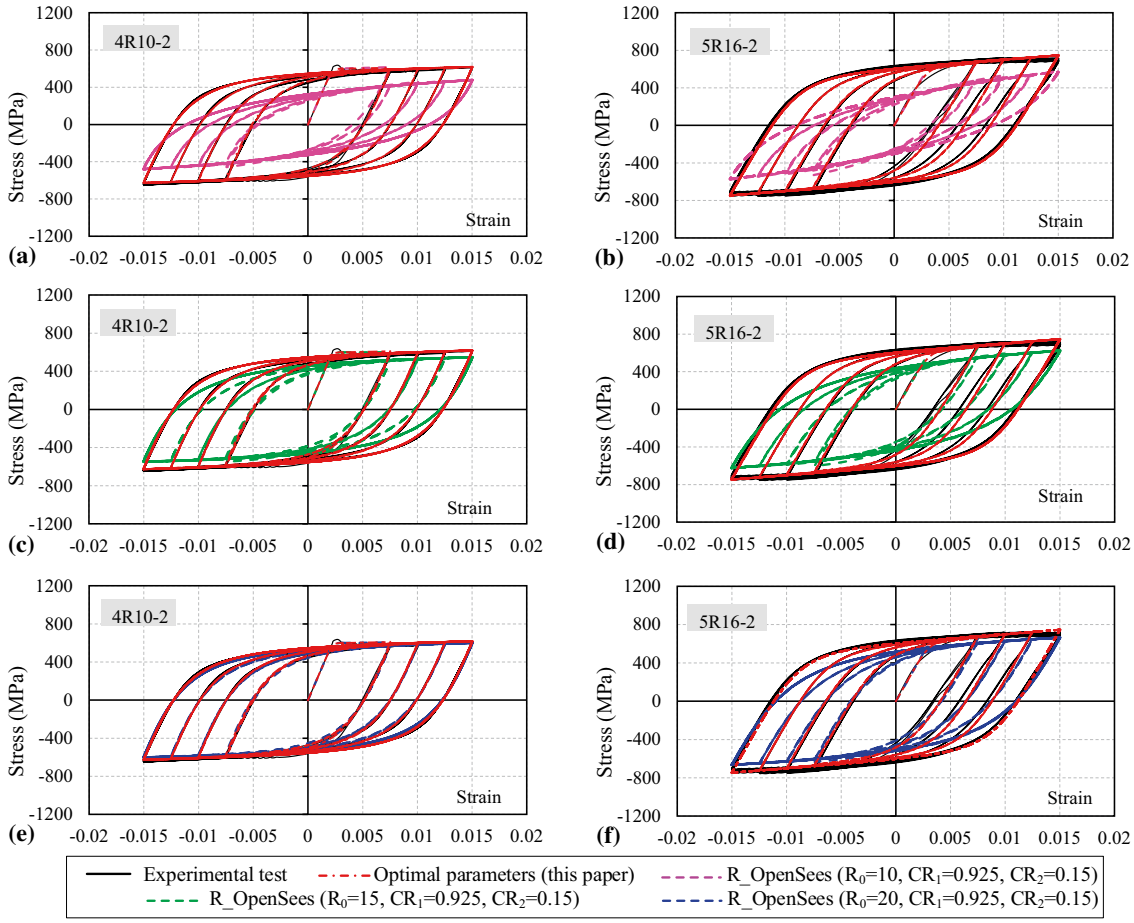

Fig. 6 Comparison among predicted behaviour (this paper), the available experimental studies, and recommended values of OpenSees (Filipou et al., 1983)

The structure is subjected to the accelerogram of the Northridge earthquake (USA, January 17, 1994, recording station: 090 CDMG Station 24,278) with the peak ground accelerations PGA = 0.568 g.

Stress–strain points of the investigated column's section are illustrated in Fig. 7 and 8. For each element, five typical cross-sections are specified for the integral calculation.

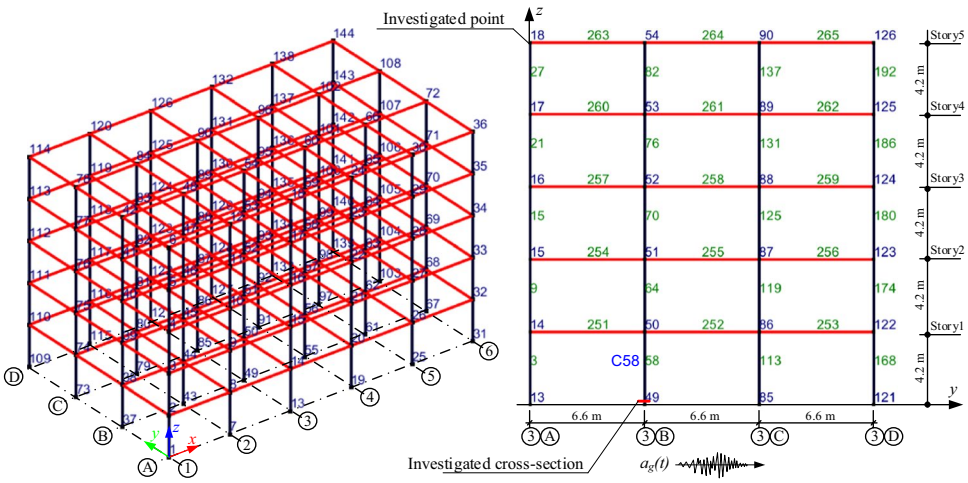

Fig. 7 Considered building structure: **a** 3D model and **b** 3rd axis elevation

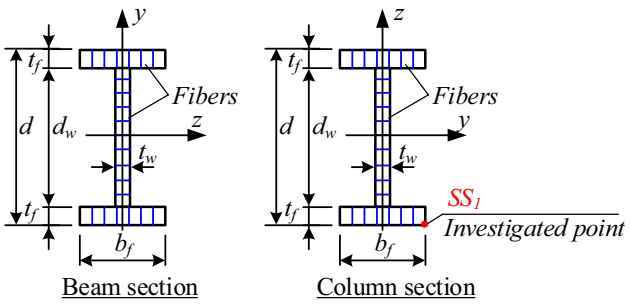

Fig. 8 Fibre model and stress–strain points for column section in OpenSees

4.2 Results and Discussions

Figure 9 shows the time-history responses of the base shear force and the horizontal displacement at the top of the building subjected to earthquake (blue line). As it is observed from Fig. 9(b), the structure presents residual displacement at the top of the building, which indicates a nonlinear behaviour of structures under the earthquake.

In order to investigate the feasibility of the optimally calibrated model for nonlinear time-history analysis of steel frame, an extensive study is conducted to compare the GMP model with optimal parameters and the model Steel01 in OpenSees (not optimal) (Mazzoni et al., 2006), which is based on the traditional bilinear model. Accordingly, three main parameters of GMP model including $E_0 = 273.8$ GPa, $f_y = 591.2$ MPa, and $b = 0.0133$ (specimen 4R10-1) are used for Steel01 model.

As it is observed in Fig. 9 and Fig. 10, the base shear forces, bending moment, and lateral displacement at the top of the structure obtained by using the Steel01 model (red dashed) are slightly higher than those of the GMP model. In the cases where the structures are subjected to stronger earthquake scenarios, these differences may be more visible, and the use of the Steel01 model may lead to significant flaws. In fact, this difference is considered a consequence of the difference between the two models Steel01 and GMP, where the transition from the elastic to the post-elastic state of material behaviour is the most notable. Further, this difference is more obvious in the post-peak response phases, suggesting that it has a significant effect on the strain energy stored in the structure.

Figure 10 presents the response history of bending moment (M_{xx}) and axial force at the bottom of column 58, axis 3-B.

The comparison of obtained results in terms of the stress–strain relationship at the investigated point SS1 (base of column 58, 3-B axis) by the two considered models is presented in Fig. 11. Specifically, Fig. 11.(a) shows the full time and Fig. 11.(b) shows the first two cycles ($t = 0$—9.95 s).

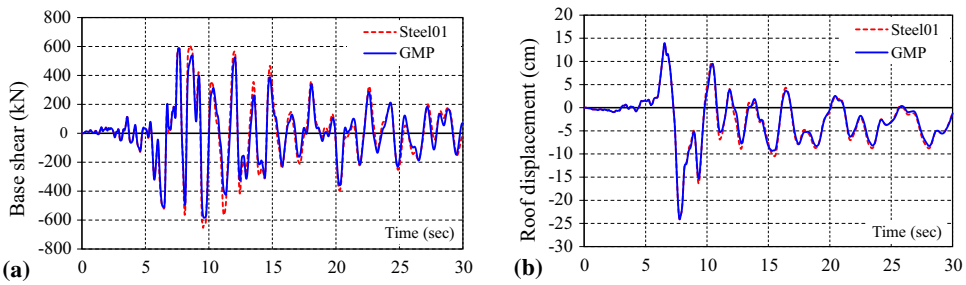

Fig. 9 Time-history responses of the structure: **a** Base shear forces and **b** Lateral displacements at the top story

As can be noticed from the above results, the two models may result in a good agreement at the peak stress–strain response. However, the behaviour during the transition of plastic-elastic deformation in both loading and unloading phases is obviously different. Consequently, the hysteresis loop shape by using the Steel01 model is a clear difference from the experimental results. From an energy point of view, the energy dissipation calculated for one cyclic may be represented by the area of the hysteresis loop of the stress–strain curve (Yang et al., 2019). Accordingly, the area of the largest hysteresis loop of the two models is used for comparison. The result shows that the Steel01 model provides a larger hysteresis loop area than that of the optimal model. This result may lead to an inaccurate assessment of energy dissipated in the structure.

Further, for lower strain, using the Steel01 model resulted in a larger prediction of the strain–stress response of the structure (green squares in Fig. 11), which may lead to significant errors in the accumulated strain energy at low strain loops. It is logical and compatible with the above findings in the response history of structures in the later periods. These comparisons are detailed in Table 3.

In the framework of this study, the optimally calibrated GMP model showed high efficiency, not only in terms of permitting automation of the analytical process but also in terms of presenting a good agreement between the numerical and experimental models. As a result, it can be considered more suitable for the seismic analysis and assessment of steel structures.

5 Conclusion

In this research, the Giuffrè-Menegotto-Pinto (GMP) model is considered to simulate the behaviour of high-strength steel. An optimal analysis method is proposed to calibrate the numerical model in order to match the experimental results. A set of ten parameters of the GMP model optimally calibrated for the numerical model are as close to the test model as possible. An extensive study was carried out to assess the recommended value by OpenSees to use with the GMP model. Obtained results are used to perform on a typical steel frame structure of a five-story building. The following is a summary of the study's main concluding remarks:

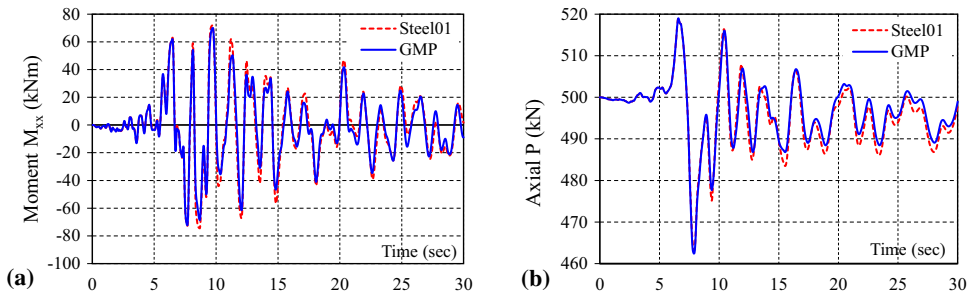

Fig. 10 Time-history responses of the structure: **a** Bending moment and **b** axial force at the bottom of Column 58, 3-B axis on the 1st floor

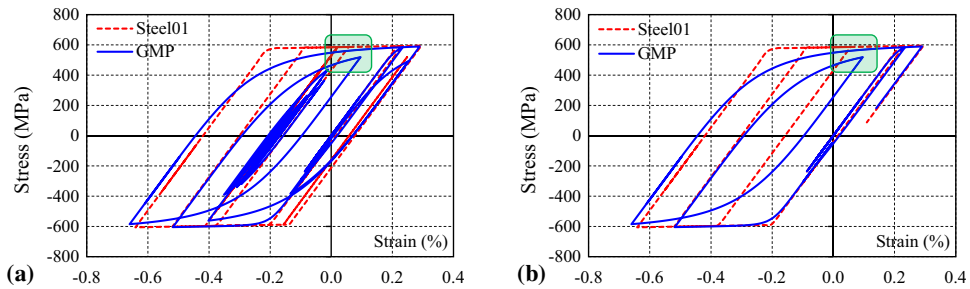

Fig. 11 The stress–strain relationship at SS1 point of Column 58/B-3 axis/ first Story: **a** the whole cycle and **b** the first three cycles

Table 3 Comparison of seismic response of considered structure between Steel01 model and optimal model

#	D_{max} (mm)	Q (kN)	E (%)	Σ (MPa)	Hysteresis area (max) per cycle (Fig. 11. (b))
Steel01	24.109	586.308	0.641	606.682	3.552
GMP	24.071	583.849	0.660	605.099	3.193
Compare (%)	0.155	0.419	2.940	0.261	10.102

- The proposed optimal analysis method shows high efficiency in calibrating the numerical model to match the test results. The difference between the calibrated model by the proposed method and the test results is found less than 10%.
- The proposed method offers a practical solution for application to open-source programs such as OpenSees, allowing the use of experimental results for analysis without the intermediate step to determine the model's parameters.
- The parameter to control the smoothness of the transition from elastic to plastic state (R_0) has an important role in adjusting the accordance of the numerical model and the tests. In the framework of this study, the suggested values of OpenSees for the GMP model proved to be inconsistent with calibration models from experimental tests of high-strength steel.
- The case study, numerical analysis of typical steel structure indicates that the use of optimally calibrated GMP model is more appropriate, while the Steel01 model may result in potential errors of cyclic nonlinear behaviour of structures.

Notwithstanding the above, this study conducted an optimal procedure to identify the parameters in a way that help the researcher optimally calibrate numerical model parameters to match the test results. Further experimental studies shall be carried out to evaluate the suitability of the method with a variety of other steels to develop an automated analysis tool oriented to OpenSees.

References

AASHTO. (2017). AASHTO LRFD Bridge Design Specifications 8th Edition. In: Washington, DC: American association of state highway and transportation officials.

Abaqus. (2014). Abaqus documentation. Retrieved from https://abaqus-docs.mit.edu/2017/English/SIMACAEEXCRefMap/simaexc-c-docproc.htm

Aghlara, R., & Tahir, M. M. (2018). A passive metallic damper with replaceable steel bar components for earthquake protection of structures. *Engineering Structures, 159*, 185–197.

AISC. (2017). *Specification for structural steel buildings*. Chicago, IL: American Institute of Steel Construction.

Anderberg, Y. (1988). Modelling steel behaviour. *Fire Safety Journal, 13*(1), 17–26.

ANSYS. (2021). ANSYS Inc. *PDF Documentation for Release, 2020*, R1.

Bauschinger, J. (1886). On the change of the elastic limit and the strength of iron and steel, by drawing out, by heating and cooling, and by repetition of loading (summary). *Minutes of Proceedings of the Institution of Civil Engineers with Other Selected and Abstracted Papers, 87*, 463.

Bosco, M., Ferrara, E., Ghersi, A., Marino, E. M., & Rossi, P. P. (2016). Improvement of the model proposed by Menegotto and Pinto for steel. *Engineering Structures, 124*, 442–456.

Bouc, R. (1967). Forced vibrations of mechanical systems with hysteresis. Paper presented at the Proceeding of the fourth conference on nonlinear oscillations, Prague.

Bu, H., He, L., & Jiang, H. (2021). Seismic fragility assessment of steel frame structures equipped with steel slit shear walls. *Engineering Structures, 249*, 113328.

Campbell, J. D., & Co-auteur, P. N. (1970). *Dynamic Plasticity of Metals: Springer*. https://doi.org/10.1007/978-3-7091-2848-0

Chaboche, J.-L. (1986). Time-independent constitutive theories for cyclic plasticity. *International Journal of Plasticity, 2*(2), 149–188.

Chan, R. W., Albermani, F., & Kitipornchai, S. (2013). Experimental study of perforated yielding shear panel device for passive energy dissipation. *Journal of Constructional Steel Research, 91*, 14–25.

Cofie, N. G., & Krawinkler, H. (1985). Uniaxial cyclic stress-strain behavior of structural steel. *Journal of Engineering Mechanics, 111*(9), 1105–1120.

CSA-S6. (2019). CSA-S6–19, Canadian highway bridge design code. In: Canadian Standards Association.

Dai Nguyen, X., & Guizani, L. (2021). Analytical and numerical investigation of natural rubber bearings incorporating U-shaped dampers behaviour for seismic isolation. *Engineering Structures, 243*, 112647.

Dunne, F., & Petrinic, N. (2005). *Introduction to computational plasticity*. London: Oxford University Press on Demand.

ECS. (2005a). Eurocode 8: Design of structures for earthquake resistance-part 1: general rules seismic actions and rules for buildings. In: European Committee for Standardization Brussels, Europe.

Filipou, F. C., Popov, E. P., & Bertero, V. V. (1983). *Effects of bond deterioration on hystereric behavior of reinforced concrete joints*. College of Engineering, University of California.

Garivani, S., Aghakouchak, A., & Shahbeyk, S. (2016). Numerical and experimental study of comb-teeth metallic yielding dampers. *International Journal of Steel Structures, 16*(1), 177–196.

Giuffrè, A. (1970). Il comportamento del cemento armato per sollecitazioni cicliche di forte intensità. Giornale del Genio Civile.

Goldberg, J. E., & Richard, R. M. (1963). Analysis of nonlinear structures. *Journal of the Structural Division, 89*(4), 333–351.

Hai, L.-T., Sun, F.-F., Zhao, C., Li, G.-Q., & Wang, Y.-B. (2018). Experimental cyclic behavior and constitutive modeling of high strength structural steels. *Construction and Building Materials, 189*, 1264–1285.

Hu, F., & Shi, G. (2018). Constitutive model for full-range cyclic behavior of high strength steels without yield plateau. *Construction and Building Materials, 162*, 596–607.

Jamkhaneh, M. E., Ebrahimi, A. H., & Amiri, M. S. (2019). Experimental and numerical investigation of steel moment resisting frame with U-shaped metallic yielding damper. *International Journal of Steel Structures, 19*(3), 806–818.

Jiao, Y., Kishiki, S., Yamada, S., Ene, D., Konishi, Y., Hoashi, Y., & Terashima, M. (2015). Low cyclic fatigue and hysteretic behavior of U-shaped steel dampers for seismically isolated buildings under dynamic cyclic loadings. *Earthquake Engineering & Structural Dynamics, 44*(10), 1523–1538.

MathWorks. (2020). Constrained Nonlinear Optimization Algorithms. Retrieved from https://www.mathworks.com

Mazzoni, S., McKenna, F., Scott, M. H., & Fenves, G. L. (2006). OpenSees command language manual. Pacific Earthquake Engineering Research (PEER) Center, 264(1), 137–158.

Menegotto, M., & Pinto, P. (1973). Method of Analysis for Cyclically Loaded RC Plane Frames Including Changes in Geometry and non-Elastic Behaviour of Elements under Combined Normal Force and Bending. Paper presented at the Proc., IABSE Symp. on resistance and ultimate deformability of structures acted on by well defined repeated loads, Zurich.

Myers, A. T. (2009). Testing and probabilistic simulation of ductile fracture initiation in structural steel components and weldments: Stanford University.

NRCC. (2015). National building code of Canada (NBCC). In: National Research Council of Canada, Associate Committee on the National Building Code.

OpenSees. (2020). The open system for earthquake engineering simulation: PEER. Retrieved from https://opensees.berkeley.edu

OpenSees. (2021). Command manual. Retrieved from https://opensees.berkeley.edu/wiki/index.php/Main_Page

OpenSeesNavigator. (2020). The Openseesnavigator: PEER. Retrieved from https://openseesnavigator.berkeley.edu/

Ramberg, W., & Osgood, W. R. (1943). Description of stress-strain curves by three parameters. Retrieved from

Real, E., Arrayago, I., Mirambell, E., & Westeel, R. (2014). Comparative study of analytical expressions for the modelling of stainless steel behaviour. *Thin-Walled Structures, 83*, 2–11.

Saeedi, F., Shabakhty, N., & Mousavi, S. R. (2016). Seismic assessment of steel frames with triangular-plate added damping and stiffness devices. *Journal of Constructional Steel Research, 125*, 15–25.

SAP2000, C.S.I (2020). *Integrated software for structural analysis & design*. Berkeley, CA, USA: Computer and Structures, Inc.

ASCE/SEI-41–13. (2014). Seismic evaluation and retrofit of existing buildings. In ASCE Standard ASCE/SEI: American Society of Civil Engineers.

Sheikhi, J., & Fathi, M. (2020). Natural rubber bearing incorporated with steel ring damper (NRB-SRD). *International Journal of Steel Structures, 20*(1), 23–34.

Taiyari, F., Mazzolani, F. M., & Bagheri, S. (2019). A proposal for energy dissipative braces with U-shaped steel strips. *Journal of Constructional Steel Research, 154*, 110–122.

Takeda, T., Sozen, M. A., & Nielsen, N. N. (1970). Reinforced concrete response to simulated earthquakes. *Journal of the Structural Division, 96*(12), 2557–2573.

TCVN-9386:2012. (2012). Vietnam national standard - design of structures for earthquake resistances. In: Ministry of Science and Technology.

Wang, M., Fahnestock, L. A., Qian, F., & Yang, W. (2017). Experimental cyclic behavior and constitutive modeling of low yield point steels. *Construction and Building Materials, 131*, 696–712.

Wang, Y.-B., Li, G.-Q., Sun, X., Chen, S., & Hai, L.-T. (2017). Evaluation and prediction of cyclic response of Q690D steel. *Proceedings of the Institution of Civil Engineers-Structures and Buildings, 170*(11), 788–803.

Wen, Y.-K. (1976). Method for random vibration of hysteretic systems. *Journal of the Engineering Mechanics Division, 102*(2), 249–263.

Yang, H., Feng, Y., Wang, H., & Jeremić, B. (2019). Energy dissipation analysis for inelastic reinforced concrete and steel beam-columns. *Engineering Structures, 197*, 109431.

Zhuge, H., Xie, X., Chen, S., & Tang, Z. (2022). Research on the multi-shear spring model for circular-section steel piers. *Journal of Constructional Steel Research, 188*, 107041.

Ziemian, R. D. (1990). *Advanced methods of inelastic analysis in the limit states design of steel structures*. USA: Cornell University.